Volume 14, Issue 2, 142420 (1-8)

Iranian Journal of Catalysis (IJC)

https://doi.org/10.57647/j.ijc.2024.1402.20

Fe_3O_4@SiO_2@NCs@Al_2O_3 as a nanocatalyst for efficient one-pot synthesis of tetrahydrobenzo[b]pyran in water

Neda Daria[1]*, Koroush Ebrahimzadeh[2,3], Naghmeh Darya[1]*

[1]*Department of Chemistry, Faculty of Science, University of Guilan, Rasht, Iran.*
[2]*Department of Education Guilan, Dr Behzad Research Institute, Rasht, Iran.*
[3]*Islamic Azad University, Sama Rasht Branch, Rasht, Iran.*

*Corresponding authors: neda.daria@yahoo.com; naghmeh.darya@yahoo.com

Review Paper

Received:
24 January 2024
Revised:
30 March 2024
Accepted:
12 May 2024
Published online:
15 June 2024

© The Author(s) 2024

Abstract:

In this research, we reported Fe_3O_4@SiO_2@NCs@Al_2O_3 [FSNCA] nanoparticles as an efficient catalyst for the synthesis of Tetrahydrobenzopyrans (THBPS) in water solvent at room temperature with short reaction time. The catalyst exhibits excellent catalytic activity, selectivity, and recyclability. The nanocatalyst structure was characterized by FT-IR, SEM, XRD, TGA, VSM, and EDS. There are significant advantages of using the FSNCA nanocatalyst such as the primary benefit is the increase in production efficiency. By enabling a one-pot synthesis process, this nanocatalyst decreases the stages required for reaction, reducing time and energy consumption. Furthermore, the possibility of recycling the catalyst contributes to economic efficiency, minimizing waste production, thereby aligning with the principles of green chemistry.

Keywords: Green chemistry; Magnetic nanocatalyst [Fe_3O_4@SiO_2@NCs@Al_2O_3]; Multicomponent reactions; Tetrahydrobenzo[b]pyran

1. Introduction

One of the fundamental principles of green chemistry is the utilization of catalysts in synthesis [1, 2]. The quest for sustainable chemical reactions has led to the development of green catalysts that offer high efficiency, selectivity, and reduced environmental impact. Nanocatalysts have emerged as a promising field due to the unique properties of nanoparticles, including large surface area, high catalytic activity, and ease of recovery [3–12].

Tetrahydrobenzo[b]pyran is an important chemical compound in the class of heterocycles, which has been considered due to its biological properties and activities such as antioxidant and antimicrobial effects. In addition, THBPS are involved in the synthesis of various reactions, making them very important in the pharmaceutical and chemical industries. They are used as drugs, anticancer agents, antibacterial agents, antifungal agents, and antiviral agents [13–25]. Due to the importance of pyrane derivatives, significant research efforts have been devoted in recent years to the development of new synthetic methods for the synthesis of these compounds. However, these methods have some drawbacks such as: long reaction times, high temperatures, tedious work-up, and in some cases, environmental pollution, and require the use of expensive devices.

As the synthesis of THBPS is a vital process in the chemical industry, the use of suitable catalysts in this process is of great importance. In this research, Fe_3O_4@SiO_2@NCs@Al_2O_3 [FSNCA] was synthesized as an efficient and recyclable nanocatalyst, and then this catalyst was successfully used in the efficient one-pot synthesis of THBPS in a green and high-yield method. The nanocatalyst used in this study consists of three different layers obtained through synthesis and coating processes. FSNCA nanocomposite is a heterogeneous catalyst that has shown excellent performance in various THBP derivatives.

FSNCA nanocatalyst consists of a magnetite core (Nano-Fe_3O_4), SiO_2 intermediate layer, nanocellulose and Al_2O_3 nanoparticles. Cellulose is a non-toxic, and biocompatible renewable raw material. Al_2O_3 provides active sites for the

synthesis of THBPS and increases the catalytic ability of the compound.

Also, using water as a solvent eliminates the need for harmful organic solvents. In addition, due to the properties of magnetite, the catalyst is easily separated at the end of the reaction, reducing waste. Also, due to the affordability of the raw materials and the high recycling rate, Fe_3O_4@SiO_2@NCs@Al_2O_3 remains a cost-effective catalyst (Scheme 1).

2. Experimental

2.1 General

The progress of the reactions was checked by thin-layer chromatography (TLC) using UV light. The products were characterized by FT-IR spectra recorded on a BRUKER-ALPHA spectrometer on a KBr disc.

2.2 Synthesis of green nanocatalyst Fe_3O_4@SiO_2@NCs@Al_2O_3 [FSNCA]

Nano-Fe_3O_4@SiO_2 was synthesized based on our previous reports in papers 1 and 2. In a flask, nanocellulose (1.000 g) was added to Water: EtOH (1:1) under stirring for 10 min. Then magnetic nanoparticles (0.5 g) were added and mixed under stirring for 1 hour at room temperature. Then, the Fe_3O_4@SiO_2@NCs were collected by an external magnet and then washed with H_2O (2×5mL). Functionalized Nano-Al_2O_3 on Fe_3O_4@SiO_2@NCs nanoparticles was prepared by the addition of the Al(O-ipr)$_3$ (1 mmol) to Fe_3O_4@SiO_2@NCs (1.000 g) and grinded at room temperature for 5 minutes. Then aloe vera extract was added to the reaction mixture and grinded at room temperature for 20 minutes. The resulting Fe_3O_4@SiO_2@NCs@Al_2O_3 was collected by an external magnet after washing with H_2O (2×5mL) and drying at room temperature (Scheme 2).

2.3 General procedure for the synthesis of THBPS derivatives(4a-4p)

In a flask, malononitrile (1 mmol), aromatic aldehyde (1 mmol), 5,5-dimethylcyclohexane-1,3-dione or 1,3-cyclohexanedione (1 mmol), FSNCA (25 mg) and H_2O (2.0 mL) were grinded at room temperature and the completion of the reaction was monitored by TLC. Then, water (5 mL) was added into the reaction mixture and the nanocatalyst was separated from the product by using an external magnet. The product was purified by recrystallization in ethanol (96%). Also, FSNCA was washed with deionized water (2×5mL) and dried at room temperature. A range of the different THBPS derivatives were synthesized with excellent yields (Table 1).

2.4 Spectral data of compound (4a)

2-amino-7,7-dimethyl-5-oxo-4-phenyl-5,6,7,8-tetrahydro-4H-chromene-3-carbonitrile (4a); IR (KBr, cm^{-1}): 3410 cm^{-1}, 3327 cm^{-1}, 2221 cm^{-1}, 1671 cm^{-1}, 1211 cm^{-1}, 742 cm^{-1}. ^{1}H NMR (500.13 MHz, DMSO); 2.07 (d, J=16.1 Hz, 1H), 2.20 (d, J=16.1 Hz, H), 2.41-2.54 (m, 2H), 4.11 (s, 1H), 6.91 (s, 2H), 7.09 (d, J=7.4 Hz, 2H), 7.17 (t, J=7.4 Hz, 1H) 7.23 (t, J=7.5 Hz, 2H). ^{13}C NMR (125.75 MHz, DMSO); 195.4, 162.4, 159.3, 144.2, 129.3, 128.0, 127.2, 121.7, 113.6, 58.4, 51.9, 34.2, 32.5, 28.2, 27.6.

3. Results and discussion

The synthesis of Fe_3O_4@SiO_2@NCs@Al_2O_3 nanocatalyst begins with the co-precipitation of iron salts, $FeCl_2$, and $FeCl_3$, this result in the formation of magnetite nanoparticles. Fe_3O_4 acts as a magnetite core in the

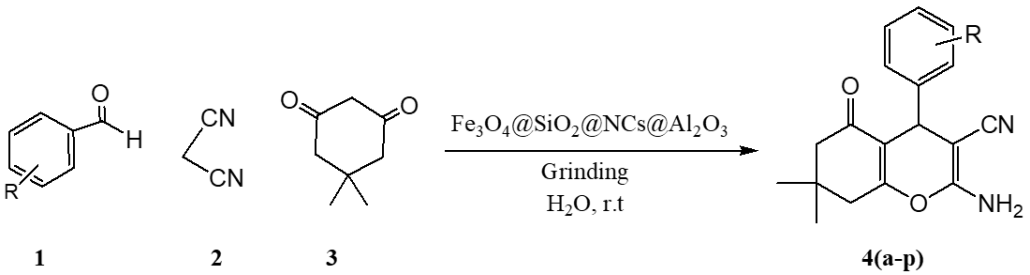

Scheme 1. Green synthesis of Tetrahydrobenzo[b]pyran using Fe_3O_4@SiO_2@NCs@Al_2O_3 as a green catalyst.

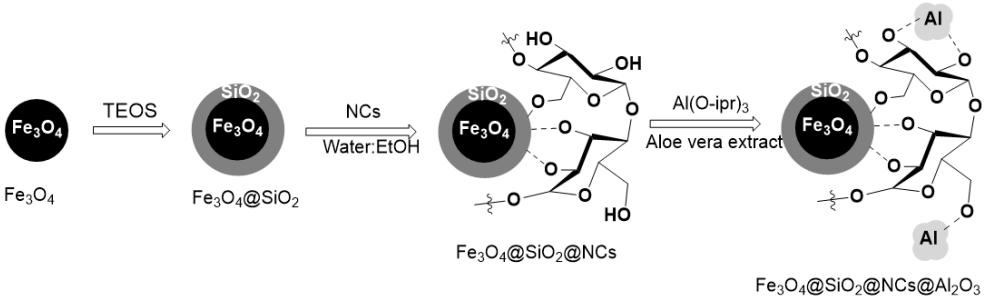

Scheme 2. Clean synthesis of multilayer magnetite Fe_3O_4@SiO_2@NCs@Al_2O_3 as a green catalyst.

Table 1. Catalyst optimization for the synthesis of THBP in H_2O at room temperature.

Entry	Catalyst	Time (min)	Yield(%)
1	FSNCA(25 mg)	10	95
2	FSNCA(20 mg)	10	92
3	FSNCA(30 mg)	10	95
5	Cellulose(25 mg)	480	—-
6	Nano-Alumina(25 mg)	10	58
7	Magnetic Cellulose(25 mg)	10	42
8	Fe_3O_4@SiO_2(25 mg)	10	36

Fe_3O_4@SiO_2@NCs@Al_2O_3 nanocatalyst for easy separation and recyclability of the catalyst. The addition of tetraethyl orthosilicate (TEOS) to the reaction mixture leads to the deposition of a layer of silica (SiO_2) around Fe_3O_4 nanoparticles. The SiO_2 shell acts as a protective layer and enhances the catalyst's durability due to its excellent thermal and chemical stability. In addition, the presence of SiO_2 provides an ideal surface for further functionalization. Nanocellulose was added to the system as a biopolymer by dispersing nanocellulose in the reaction mixture, NCs a natural polymer, serves as a linker material in the Fe_3O_4@SiO_2@NCs@Al_2O_3 nanocatalyst. Its unique structure and abundant hydroxyl groups enable strong interaction with both the Fe_3O_4 core and SiO_2 shell. This linker role enhances the stability of the overall nanocatalyst, preventing the separation of active species during catalytic reactions. Finally, the addition of the Al(O-ipr)$_3$, allows the deposition of an alumina layer (Al_2O_3) on Fe_3O_4@SiO_2@NCs nanoparticles. The presence of Al_2O_3 contributes to the mechanical strength, and durability of the nanocatalyst and in enhancing the overall activity of this nanocatalyst, which makes it especially suitable for catalytic reactions. It also provides sites for reactions, thus increasing the overall catalytic activity. The resulting catalyst exhibits a core-shell structure, with magnetite, silica, nanocellulose, and alumina layers, offering unique properties for various catalytic applications. The catalyst structure was characterized by SEM (Figure 1), FT-IR (Figure 2 (a-c)), XRD (Figure 3 (a-c)), EDS (Figure 4), VSM (Figure 5 (a-c)) and TGA (Figure 6).

3.1 Scanning electron microscope (SEM) analysis

First, the catalyst morphology was analyzed by SEM (Figure 1). The SEM image and histogram confirmed that they exist as core-shell structures with an average size range of 44 nm.

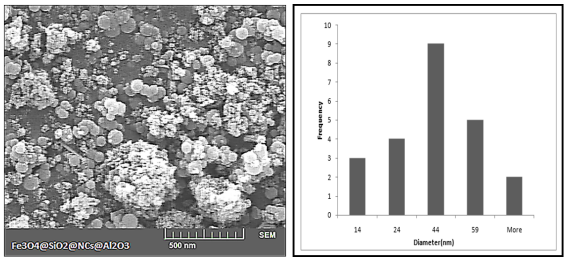

Figure 1. Scanning electron microscope (SEM) and histogram of Fe_3O_4@SiO_2@NCs@Al_2O_3 nanocatalyst.

3.2 FT-IR analysis

The FT-IR spectra of (a)Fe_3O_4 (b)Fe_3O_4@SiO_2 and (c)Fe_3O_4@SiO_2@NCs@Al_2O_3 were recorded and are given below (Figure 2 (a-c)). The Fe-O bond stretching appeared at around 400-600 cm^{-1} in Fe_3O_4 magnetite nanoparticles and the absorbance peaks at around 1114cm^{-1} are assigned to Si-O in silicon dioxide groups (Figure 2 (a-b)). After the immobilization of Al_2O_3 NPs on Fe_3O_4@SiO_2@NCs (Figure 2 c), a broad band at 3000-3500 cm^{-1} is assigned to the stretching vibrations of O-H groups. The absorption bands at 1000-1200 cm^{-1} are assigned to stretching vibrations of C-O bonds in nanocellulose and Si-O-C in silicon dioxide groups which coated by nanocellulose. The absorption band around 400-600 cm^{-1} are assigned to Fe-O bond stretching in Fe_3O_4 magnetite nanoparticles. Also, the absorption band around 700-1000 cm^{-1} are assigned to the Al-O-C band for Al_2O_3 attached to nanocellulose.

3.3 X-ray Diffraction Spectroscopy (XRD) analysis

Fe_3O_4@SiO_2@NCs@Al_2O_3 nanoparticles were analyzed by X-ray Diffraction Spectroscopy (XRD) (Figure 3 (a–c)). The XRD pattern clearly shows the structure of the catalyst. The diffraction peaks at around 18.3°, 30°, 35.4°, 43.05°, 53.4°, 56.9°, and 62.5° are corresponded to the (1 1 1), (2 2 0), (3 1 1), (4 0 0), (4 2 2), (5 1 1) and (4 4 0) surfaces, which are readily recognized in the XRD patterns and show good agreement with the cubic structure of Fe_3O_4 (JCPDS File No. 19-0626). The presence of amorphous SiO_2 is clearly indicated by a broad signal around 22.5°, suggesting that the nanoparticles are coated with silica. The diffraction

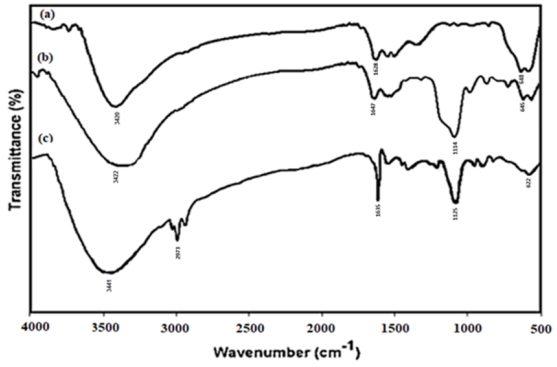

Figure 2. FT-IR spectrum of (a) Fe_3O_4, (b) Fe_3O_4@SiO_2, (c) Fe_3O_4@SiO_2@NCs@Al_2O_3.

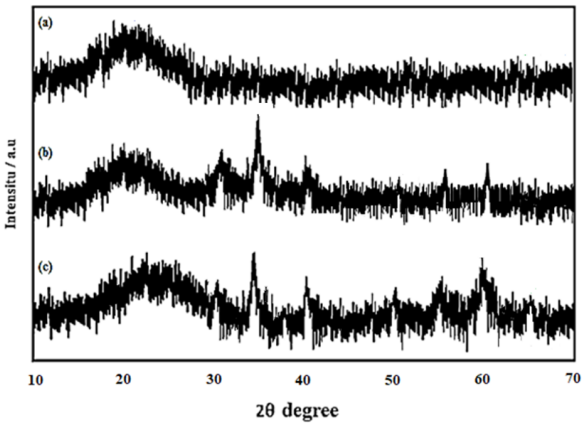

Figure 3. XRD patterns of (a) SiO_2, (b) Fe_3O_4@SiO_2, (c) Fe_3O_4@SiO_2@NCs@Al_2O_3.

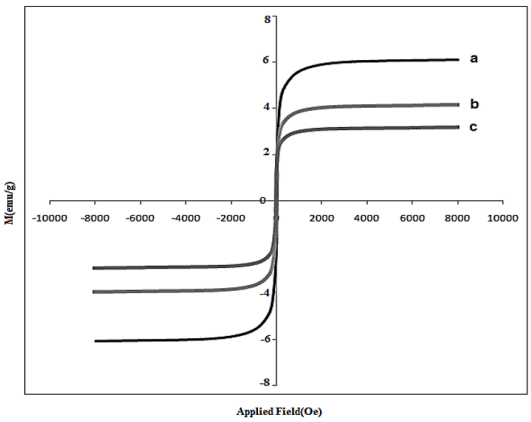

Figure 5. VSM diagram (a) Fe_3O_4, (b) Fe_3O_4@SiO_2(c) Fe_3O_4@SiO_2@NCs@Al_2O_3.

peaks 16.44 and 22.17 indicate the presence of nanocellulose. Also, the diffraction peaks at 35.1°, 37.8°, 43.4°, 57.5°, and 66.5° correspond to the (1 0 4), (1 1 0), (1 1 3), (1 1 6), and (2 1 4)) surfaces and showing good agreement with the rhombohedral (corundum) alumina phase (JCPDS File No. 46-1212).

3.4 EDS analysis

In the EDS analysis (Figure 4) clearly indicates the presence of iron, oxygen, silicon, carbon, and aluminum in the structure of the catalyst. Therefore, the above results fully confirmed the synthesis of the nanocatalyst.

3.5 VSM analysis

In the VSM analysis of the nanocatalyst [Fe_3O_4@SiO_2@NCs@Al_2O_3] (Figure 5 (a–c)), the nanocatalyst exhibited a superparamagnetic behavior due to zero remanence since the hysteresis loop was not observed. The magnetic property of the nanocatalyst is sufficient for separation using a simple external magnet. According to (Figure 5 a), the highest saturation magnetization belongs to Fe_3O_4nanoparticles. In addition, the curves showed a decrease in saturation magnetic values for Fe_3O_4@SiO_2. The lower MS value for Fe_3O_4@SiO_2 is due to the presence of non-magnetic silica on the surface of the Fe_3O_4 nanoparticles [26–28]. It confirms that silica nanoparticles bond on the surface of Fe_3O_4 nanoparticles and the non-magnetic SiO_2 layer is coated on the Fe_3O_4nanoparticles. It indicates the layer-by-layer coating and the successful synthesis of the Fe_3O_4@SiO_2@NCs@Al_2O_3 nanocatalyst.

3.6 Thermal analysis (TGA)

According to the TGA analysis (Figure 6), the stability of Fe_3O_4@SiO_2@NCs@Al_2O_3 nanoparticles was observed up to 400-600 °C. Additionally, the TGA indicates an initial weight loss due to moisture evaporation from the sample. The main weight loss step in the temperature occurs within the range of 200-350 °C, which corresponds to the decomposition of the NCs units on the nanocatalyst. The weight loss at 400 °C temperature is attributed to the thermal crystal phase transformation. Additionally, the presence of nanocellulose and alumina layers provides excellent stability of the nanocatalyst under harsh reaction conditions.

3.7 Catalytic activity

To investigate the ability of this catalyst, the three-component reaction involving benzaldehyde (1), malononitrile (2). and dimedone (3) was chosen as a model reaction to produce THBP (4a) (Scheme 3). Then, the reaction conditions were optimized by various catalysts and solvents

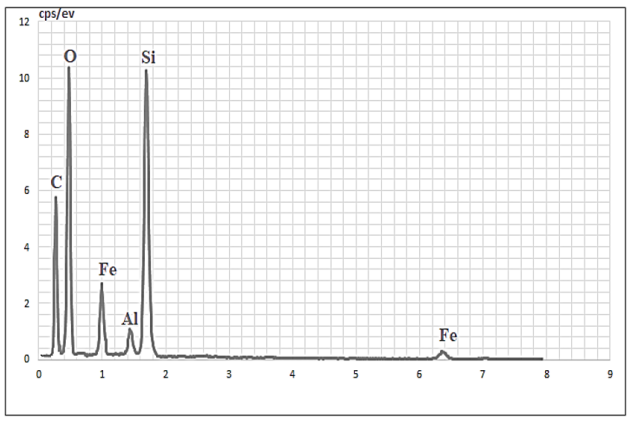

Figure 4. EDS spectrum of Fe_3O_4@SiO_2@NCs@Al_2O_3.

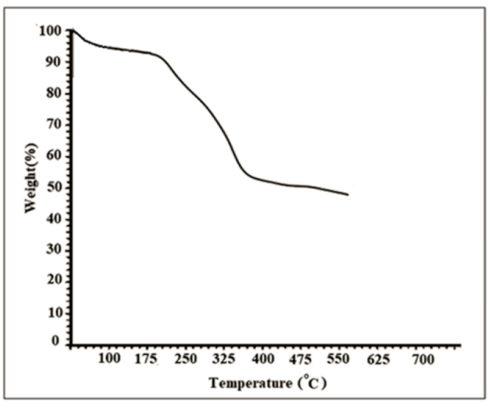

Figure 6. TGA analysis of Fe_3O_4@SiO_2@NCs@Al_2O_3.

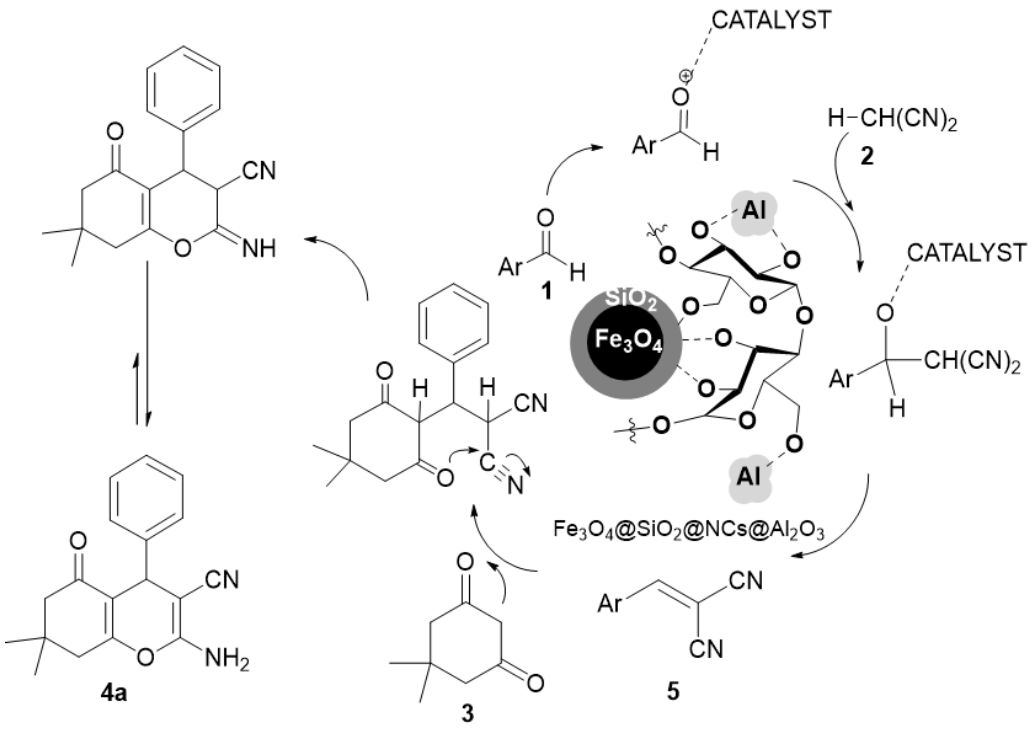

Scheme 3. Green synthesis of THBPS by using FSNCA nanocatalyst.

(Table 1, Table 2). This nanocatalyst exhibited high selectivity, excellent yield (95%), efficiency, and high purity in a short reaction time (10 minutes), green solvent (H_2O), and low temperature (room temperature). After identifying the optimal conditions, other pyran derivatives were synthesized using the catalyst (Table 3).

3.8 Suggested mechanism for the synthesis of THBPS by using green catalyst Fe_3O_4@SiO_2@NCs@Al_2O_3

The mechanism involves the formation of intermediate 5, followed by the cyclization, subsequent neutralization, and tautomerization to yield THBPS compounds. The unique structure and composition of the green catalyst [Fe_3O_4@SiO_2@NCs@Al_2O_3] facilitate the key steps of this mechanism, leading to enhanced reaction efficiency and selectivity (Scheme 3).

3.9 Catalyst stability and recyclability

Catalyst recyclability is a critical factor in the development of sustainable and environmentally friendly processes. The Fe_3O_4@SiO_2@NCs@Al_2O_3nanocatalyst exhibited excellent recyclability, with no significant loss in catalytic activity even after multiple cycles (Figure 7). The nanocatalyst could be separated using a simple external magnet. This feature not only reduces waste generation but also lowers the overall cost of production.

Table 2. Solvents effect in the synthesis of THBP by FSNCA at room temperature at 10 min.

Entry	Solvent	Yield (%)
1	Solvent-free	92
2	H_2O	95
3	EtOH/H_2O	90
4	EtOH	84
5	Ethyl acetate	80

3.10 Hot filtration test

A hot filtration test for Dimedone (1 mmol), benzaldehyde (1 mmol), and malononitrile (1 mmol) model reaction was performed by FSNCA-Catalyst (25 mg). Then, the catalyst was separated and the reaction mixture was monitored and it was found that there was almost no further conversion after catalyst separation. The results clearly confirmed that the nanocatalyst is stable under artificial conditions and can be reused several times without reducing the catalytic activity (Figure 7).

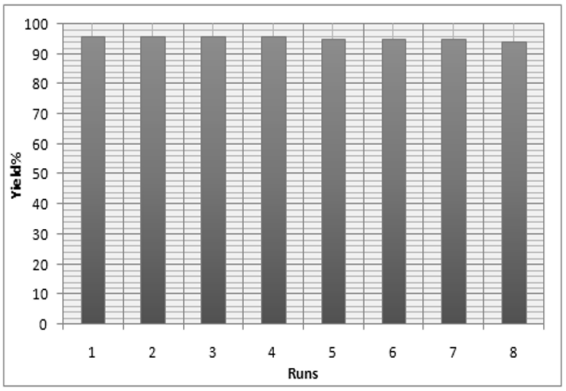

Figure 7. Catalyst reusability.

Table 3. One-pot synthesis of THBPS[a,b] derivatives by using FSNCA.

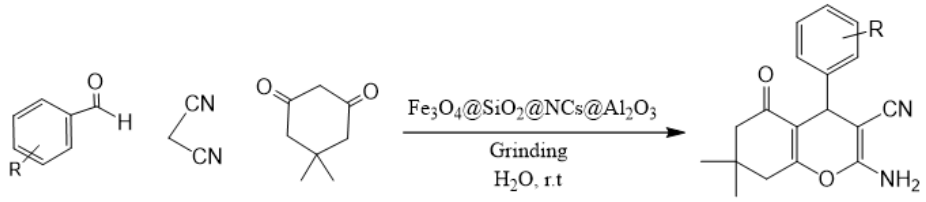

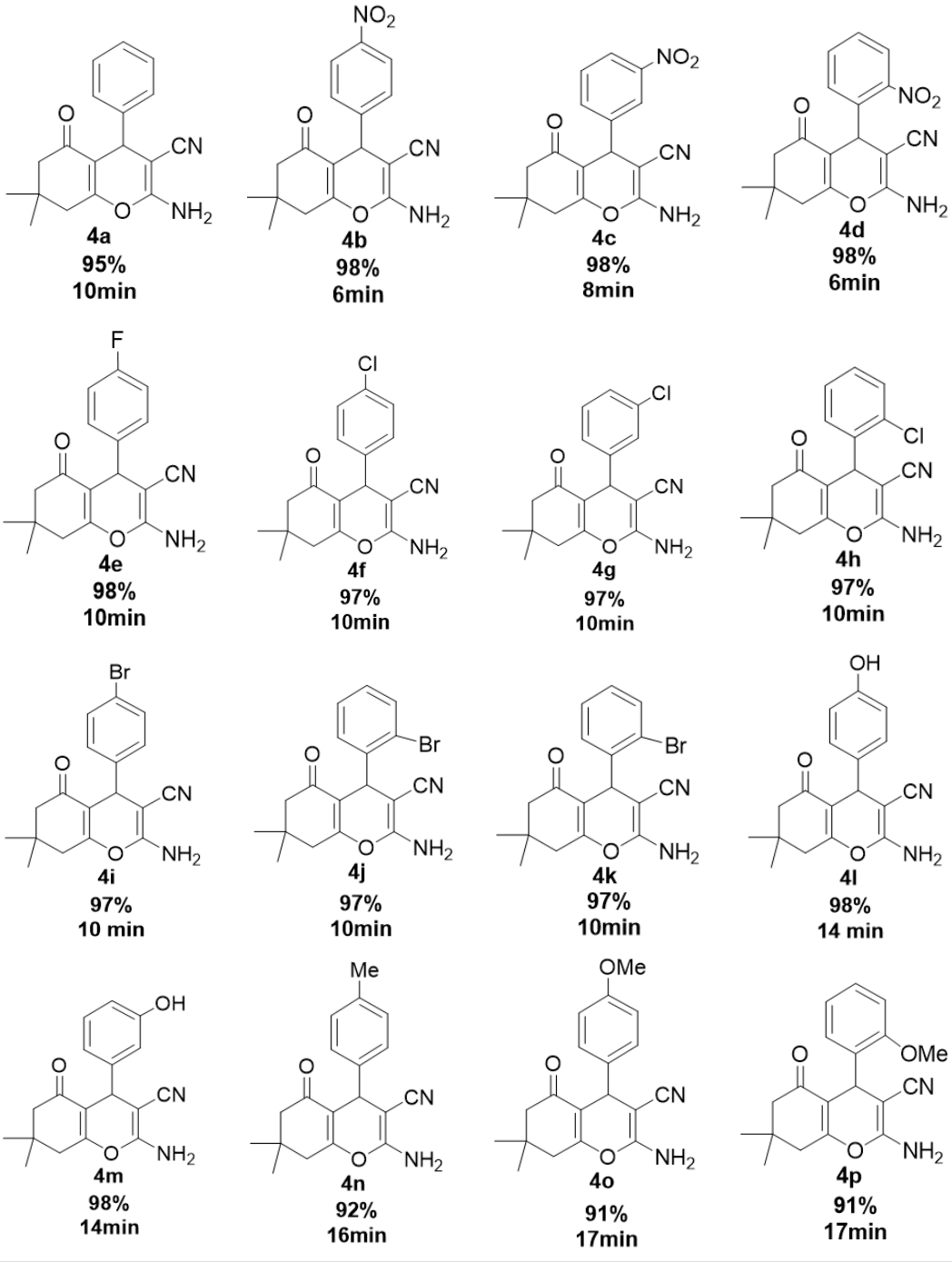

[a] Reaction conditions: dimedone (1mmol), benzaldehyde (1mmol), malononitrile (1mmol), FSNCA (25 mg), green catalyst / room temperature, H_2O.
[b] Isolated yield.

Table 4. Comparison of the catalytic efficiency of FSNCA green catalyst to some reported catalysts for the synthesis of Tetrahydrobenzo[b]pyran.

Entry	Catalyst	Solvent	Conditions	Time (min)	Yield (%)	Ref
1	**FSNCA**	**H_2O**	**r.t**	**10**	**95**	**this work**
2	$PhB(OH)_2$	$EtOH/H_2O$	Reflux	30	88	[29]
3	$Fe_3O_4@SiO_2@TiO_2$	Solvent-free	95 °C	20	93	[30]
4	Thiamine mononitrate	Water: ethanol	Ultrasonication	20	82	[31]
5	$Ce_1Mg_xZr_{1-x}O_2$	Ethanol	Reflux	35	91	[32]
6	Sodium bromide	Solvent free	Microwave /70 °C	10	95	[33]
7	$CA\text{-}SiO_2$	$EtOH/H_2O$	Reflux	17	93	[34]
8	CuO decorated on CNs	Water	r.t	20	97	[35]

3.11 Comparison of the catalytic efficiency of $Fe_3O_4@SiO_2@NCs@Al_2O_3$ with other reported catalysts for the synthesis of THBPS

According to Table 4, $Fe_3O_4@SiO_2@NCs@Al_2O_3$ has emerged as an ideal catalyst for the green synthesis of THBPS due to its unique properties. $Fe_3O_4@SiO_2@NCs@Al_2O_3$ exhibits superior performance in terms of green reaction conditions, green solvent (H_2O), reaction temperature (room temperature), reaction time (10 minutes), product's purity and excellent efficiency (95%), one-pot grinding-methodology, the absence of side reactions, recovery and reusability of the nanocatalyst. Environmentally friendly, availability, high efficiency, short reaction time, mild reaction conditions, stability and recyclability of the catalyst, and clean separation of the catalyst are the most important features of this method compared to previously reported catalysts.

4. Conclusion

$Fe_3O_4@SiO_2@NCs@Al_2O_3$ (FSNCA) nanocatalyst offers a sustainable and efficient approach for the synthesis of the Tetrahydrobenzo[b]pyran (THBPS). The unique combination of magnetite, silica, nanocellulose, and alumina provides enhanced catalytic properties and easy separation and recyclability, making it an ideal catalyst for green organic synthesis. The development and application of this green catalyst pave the way for the development of more sustainable and environmentally friendly chemical processes.

Acknowledgments
We gratefully acknowledge of Department of Education Guilan, Dr. Behzad Research Institute, Islamic Azad University, Sama Rasht Branch, and University of Guilan.

Authors Contributions
Authors have equal contribution role in preparing the paper.

Availability of Data and Materials
The data that support the findings of this study are available from the corresponding author upon reasonable request.

Conflict of Interests
The authors declare that they have no known competing financial interests or personal relationships that could have appeared to influence the work reported in this paper.

Open Access
This article is licensed under a Creative Commons Attribution 4.0 International License, which permits use, sharing, adaptation, distribution and reproduction in any medium or format, as long as you give appropriate credit to the original author(s) and the source, provide a link to the Creative Commons license, and indicate if changes were made. The images or other third party material in this article are included in the article's Creative Commons license, unless indicated otherwise in a credit line to the material. If material is not included in the article's Creative Commons license and your intended use is not permitted by statutory regulation or exceeds the permitted use, you will need to obtain permission directly from the OICC Press publisher. To view a copy of this license, visit https://creativecommons.org/licenses/by/4.0.

References

[1] N. Darya and H. Tajik. . *Iran. J. Catal*, **11**(2021): 317–329, .

[2] N. Darya and H. Tajik. *Synth. Commun*, **51**(2021):3546–3564, . DOI: https://doi.org/10.1080/00397911.2021.1959614.

[3] S. Sajjadifar, I. Amini, and M. Karimian. *Iran. J. Catal*, **11**(2021):59–67.

[4] E. Babaei and B. Mirjalili. *Iran. J. Catal*, **10**(2020): 219–226.

[5] V. Khorramabadi, D. Habibi, and S. Heydari. *Org Prep Proced Int*, **52**(2020):139–146. DOI: https://doi.org/10.1080/00304948.2020.1716624.

[6] J. Safaei-Ghomi and R. Teymuri. . *Iran. J. Catal*, **11**(2021):113–123.

[7] N. Hazeri, S. Salahi, M. Lashkari, M. Maghsoodlou, E. Esmaeili-Shahri, and E. Molashahi. . *Org Prep Proced Int*, **50**(2018):375–383. DOI: https://doi.org/10.1080/00304948.2018.1462077.

[8] M. Jafarpour, A. Rezaeifard, M. Ghahramaninezhad, and F. Feizpour. . *Green Chem*, **17**(2015):442–452. DOI: https://doi.org/10.1039/C4GC01398K.

[9] M. Hakimi and M. Alikhani. *Inorg. Organomet. Polym. Mater*, **30**(2020):504–512. DOI: https://doi.org/10.1007/s10904-019-01210-3.

[10] M. Blanco, D. Mosconi, C. Tubaro, A. Biffis, D. Badocco, P. Pastore, M. Otyepka, A. Bakandritsos, Zh. Liu, W. Ren, S. Agnoli, and G. Granozzi. . *Green Chem*, **21**(2019):5238–5247. DOI: https://doi.org/10.1039/C9GC01436E.

[11] N. Khatun, A. Gogoi, P. Basu, P. Das, and B.K. Patel. . *RSC Adv*, **4**(2014):4080–4084. DOI: https://doi.org/10.1039/C3RA45298K.

[12] Y. Zhao, Y. Kang, H. Li, and H. Li. *Green Chem*, **20**(2018):2781–2787. DOI: https://doi.org/10.1039/C8GC00743H.

[13] S. Gurumurthi, V. Sundari, and R. Valliappan. *E- J. Chem*, **6**(2009):466–472. DOI: https://doi.org/10.1155/2009/875086.

[14] I. Devi and P.J. Bhuyan. . *Tetrahedron Lett*, **45**(2004):8625–8627, . DOI: https://doi.org/10.1016/j.tetlet.2004.09.158.

[15] L. Fotouhi, M.M. Heravi, A. Fatechi, and K. Bakhtiari. . *Tetrahedron Lett*, **48**(2007):5379–5381. DOI: https://doi.org/10.1016/j.tetlet.2007.06.035.

[16] T.S. Jin, A.Q. Wang, X. Wang, J.S. Zhang, and T.S. Li. . *Synlett*, **5**(2004):0871–0873. DOI: https://doi.org/10.1055/s-2004-820025.

[17] D. Shi, J. Mou, Q. Zhuang, and X. Wang. . *J Chem Res*, **12**(2004):821–823. DOI: https://doi.org/10.3184/0308234043431294.

[18] S. Balalaie, M. Bararjanian, A.M. Amani, and B. Movassagh. . *Synlett*, **02**(2006):263–266. DOI: https://doi.org/10.1055/s-2006-926227.

[19] L.M. Wang, J.H. Shao, H. Tian, Y.H. Wang, and B. Liu. . *J. Fluorine. Chem*, **127**(2006):97–100, . DOI: https://doi.org/10.1016/j.jfluchem.2005.10.004.

[20] Gowravaram Sabitha, K. Arundhathi, K. Sudhakar, B. S. Sastry, and J. S. Yadav. . *Synth. Commun*, **39**(2009):433–442. DOI: https://doi.org/10.1080/00397910802378399.

[21] X. Wang, D. Shi, S. Tu, and C. Yao. . *Synth. Commun*, **33**(2003):119–126, . DOI: https://doi.org/10.1081/SCC-120015567.

[22] M. Seifi and H. Sheibani. . *Catal. Lett*, **126**(2008): 275–279. DOI: https://doi.org/10.1007/s10562-008-9603-5.

[23] B. Maleki and S.S. Ashrafi. . *RSC Adv*, **4**(2014):42873–42891. DOI: https://doi.org/10.1039/C4RA07813F.

[24] P.L. Anandgaonker, S. Jadhav, S.T. Gaikwad, and A.S. Rajbhoj. . *J. Clust. Sci*, **25**(2014):483–493. DOI: https://doi.org/10.1007/s10876-013-0626-8.

[25] X.S. Wang, D.Q. Shi, S.J. Tu, and C.S. Yao. . *Synth. Commun. Now*, **33**(2003):119–126, . URL 10.1081/SCC-120015567.

[26] W.F. Elmobarak and F. Almomani. . *Chemosphere*, **265**(2021):129054. DOI: https://doi.org/10.1016/j.chemosphere.2020.129054.

[27] A.Gemeay, B.E. Keshta, R.G. Sharkawy, and A. Zaki. . *Environ. Sci. Pollut. Res. Int*, **27**(2020):32341–32358. DOI: https://doi.org/10.1007/s11356-019-06530-y.

[28] R.K. Sharma, Y.Monga, and A. Puri. . *J. Mol. Catal. A Chem*, **393**(2014):84–95. DOI: https://doi.org/10.1016/j.molcata.2014.06.009.

[29] S. Nemouchi, R. Boulcina, B. Carboni, A. Debache, and C.R. Chimie. . *Polyhedron*, **15**(2012):394–397. DOI: https://doi.org/10.1016/j.crci.2012.01.003.

[30] A. Khazaei, F. Gholami, V. Khakyzadeh, A.R. Moosavi-Zare, and J. Afsar. . *RSC Adv*, **5**(2015):14305–14310. DOI: https://doi.org/10.1039/C4RA16300A.

[31] A.U. Khandebharad, S.R. Sarda, Ch.H. Gill, Mahesh, G. Soni, and B.R. Agrawal. . *Res Chem Intermed*, **42**(2016):5779–5787. DOI: https://doi.org/10.1007/s11164-015-2403-9.

[32] S. Rathod, B. Arbad, and M. Lande. . *Chin. J. Catal*, **31**(2010):631–636. DOI: https://doi.org/10.1016/S1872-2067(09)60078-4.

[33] I. Devi and P. Bhuyan. *Tetrahedron Lett*, **45**(2004):8625–8627, . DOI: https://doi.org/10.1016/j.tetlet.2004.09.158.

[34] H. Abdi Oskooie, M.M. Heravi, N. Karimi, and M. Ebrahim Zadeh. . *Synth. Commun*, **41**(2011):436–440. DOI: https://doi.org/10.1080/00397911003587499.

[35] C. Thanaraj, G.R. Priya Dharsini, N. Ananthan, and R. Velladurai. . *Inorg. Nano-Met. Chem*, **49**(2019):313–321. DOI: https://doi.org/10.1080/24701556.2019.1661459.